RBF-Partition of Unity Method: an overview of recent results

Alessandra De Rossi[a]

In collaboration with
Roberto Cavoretto[a], Emma Perracchione[b]

[a]Department of Mathematics "G. Peano"
University of Torino – Italy
[b]Department of Mathematics "T. Levi-Civita"
University of Padova – Italy

Localized Kernel-Based Meshless Methods for PDEs
ICERM, Providence, Rhode Island

Acknowledgements

- This talk gives an overview about the Partition of Unity (PU) interpolation, locally implemented by means of Radial Basis Functions (RBFs), and proposes some original investigations.

- Other co-authors: Stefano De Marchi (University of Padova, Italy); Greg Fasshauer (Colorado School of Mines, Golden, CO); Gabriele Santin (University of Stuttgart, Germany); Ezio Venturino (University of Torino, Italy).

- Funds: Department of Mathematics "G. Peano" via the projects "Metodi numerici nelle scienze applicate" (Principal Investigator (PI) A. D.), "Metodi e modelli numerici per le scienze applicate" (PI A. D.), European Cooperation in Science and Technology (ECOST), Gruppo Nazionale per il Calcolo Scientifico (GNCS–INdAM).

- These researches have been accomplished within RITA (Rete ITaliana di Approssimazione).

Outline

- Preliminaries: RBF-PUM interpolation.
- Improvements of the RBF-PUM:
  - efficiency;
  - accuracy;
  - positivity;
  - stability.
- Approximation of track data via RBF-PUM.

Essential references

Preliminaries: RBF-PUM interpolation


I. Babuška, J.M. Melenk, *The partition of unity method*, Int. J. Numer. Meth. Eng. **40** (1997), 727–758.


M.D. Buhmann, *Radial Basis Functions: Theory and Implementation*, Cambridge Monogr. Appl. Comput. Math., vol. 12, Cambridge Univ. Press, Cambridge, 2003.


G.E. Fasshauer, *Meshfree Approximations Methods with* MATLAB, World Scientific, Singapore, 2007.


G.E. Fasshauer, M.J. McCourt, *Kernel-based Approximation Methods Using* MATLAB, World Scientific, Singapore, 2015.


H. Wendland, *Scattered Data Approximation*, Cambridge Monogr. Appl. Comput. Math., vol. 17, Cambridge Univ. Press, Cambridge, 2005.


H. Wendland, *Fast evaluation of radial basis functions: Methods based on partition of unity*, in: C.K. Chui et al. (Eds.), Approximation Theory X: Wavelets, Splines, and Applications, Vanderbilt Univ. Press, Nashville, 2002, 473–483.

Statement of the problem

Problem

Given $\mathcal{X}_N = \{\boldsymbol{x}_i, i = 1, \ldots, N\} \subseteq \Omega$ a set of distinct data points (or data sites or nodes), arbitrarily distributed on a domain $\Omega \subseteq \mathbb{R}^M$, with an associated set $\mathcal{F}_N = \{f_i = f(\boldsymbol{x}_i), i = 1, \ldots, N\}$ of data values (or measurements or function values), which are obtained by sampling some (unknown) function $f : \Omega \longrightarrow \mathbb{R}$ at the nodes $\boldsymbol{x}_i$, the scattered data interpolation problem consists in finding a function $R : \Omega \longrightarrow \mathbb{R}$ such that

$$R(\boldsymbol{x}_i) = f_i, \quad i = 1, \ldots, N.$$

Here, we consider RBFs and thus the interpolant is expressed as

$$R(\boldsymbol{x}) = \sum_{k=1}^{N} c_k \phi(\|\boldsymbol{x} - \boldsymbol{x}_k\|_2), \quad \boldsymbol{x} \in \Omega.$$

Uniqueness of the solution

- The problem reduces to solving a linear system $A\boldsymbol{c} = \boldsymbol{f}$, where the entries of A are given by

$$(A)_{ik} = \phi\left(\|\boldsymbol{x}_i - \boldsymbol{x}_k\|_2\right), \quad i,k = 1,\ldots,N.$$

- Moreover, the problem is well-posed under the assumption that ϕ is strictly positive definite. We remark that the uniqueness of the interpolant can be ensured also for the general case of strictly conditionally positive definite functions, by adding a polynomial term.

- In what follows, we might also refer to the more general case for which $\Phi : \mathbb{R}^M \times \mathbb{R}^M \longrightarrow \mathbb{R}$ is a strictly positive definite kernel, i.e. the entries of A are given by

$$(A)_{ik} = \Phi\left(\boldsymbol{x}_i, \boldsymbol{x}_k\right), \quad i,k = 1,\ldots,N.$$

Examples of RBFs

- In Table 1, we summarize several RBFs. Note that r denotes the euclidean distance and ε the shape parameter.

Table 1: Examples of RBFs.

$\phi(r) = e^{-(\varepsilon r)^2}$	Gaussian C^∞	G
$\phi(r) = (1 + (\varepsilon r)^2)^{-1/2}$	Inverse MultiQuadric C^∞	IMQ
$\phi(r) = e^{-\varepsilon r}$	Matérn C^0	M0
$\phi(r) = e^{-\varepsilon r}(1 + \varepsilon r)$	Matérn C^2	M2
$\phi(r) = e^{-\varepsilon r}(3 + 3\varepsilon r + (\varepsilon r)^2)$	Matérn C^4	M4
$\phi(r) = (1 - \varepsilon r)_+^2$	Wendland C^0	W0
$\phi(r) = (1 - \varepsilon r)_+^4 (4\varepsilon r + 1)$	Wendland C^2	W2
$\phi(r) = (1 - \varepsilon r)_+^6 (35(\varepsilon r)^2 + 18\varepsilon r + 3)$	Wendland C^4	W4

Reproducing kernels and Hilbert spaces

Definition

The space $\mathcal{N}_\Phi(\Omega) = \overline{\text{span}\{\Phi(\cdot, \boldsymbol{x}), \boldsymbol{x} \in \Omega\}}$, equipped with the bilinear form $(\cdot,\cdot)_{\overline{H_\Phi(\Omega)}}$ defined as

$$\left(\sum_{i=1}^{m} c_i \Phi(\cdot, \boldsymbol{x}_i), \sum_{k=1}^{n} d_k \Phi(\cdot, \boldsymbol{x}_k)\right)_{\overline{H_\Phi(\Omega)}} = \sum_{i=1}^{m}\sum_{k=1}^{n} c_i d_k \Phi(\boldsymbol{x}_i, \boldsymbol{x}_k).$$

is known as native space of Φ.

Definition

The separation and fill distances, which are a measure of data distribution, are respectively given by

$$q_{\mathcal{X}_N} = \frac{1}{2}\min_{i\neq k} \|\boldsymbol{x}_i - \boldsymbol{x}_k\|_2, \quad h_{\mathcal{X}_N} = \sup_{\boldsymbol{x}\in\Omega}\left(\min_{\boldsymbol{x}_k\in\mathcal{X}_N} \|\boldsymbol{x} - \boldsymbol{x}_k\|_2\right).$$

Error bounds for RBF interpolants

Theorem

Suppose $\Omega \subseteq \mathbb{R}^M$ is open and bounded and satisfies an interior cone condition and let $\Phi \in C^{2k}(\Omega \times \Omega)$ be symmetric and strictly conditionally positive definite of order L. Fix $\boldsymbol{\alpha} \in \mathbb{N}_0^M$ with $|\boldsymbol{\alpha}| \leq k$. Then there exist positive constants h_0 and C independent of $\boldsymbol{x}$, f and Φ, such that

$$|D^{\boldsymbol{\alpha}} f(\boldsymbol{x}) - D^{\boldsymbol{\alpha}} R(\boldsymbol{x})| \leq C h_{\mathcal{X}_N}^{k-|\boldsymbol{\alpha}|} \sqrt{C_\Phi(\boldsymbol{x})} |f|_{\mathcal{N}_\Phi(\Omega)},$$

provided $h_{\mathcal{X}_N} \leq h_0$ and $f \in \mathcal{N}_\Phi(\Omega)$, where

$$C_\Phi(\boldsymbol{x}) = \max_{|\boldsymbol{\beta}|+|\boldsymbol{\gamma}|=2k} \left(\max_{\boldsymbol{w},\boldsymbol{z} \in \Omega \cap B\left(\boldsymbol{x}, C_2 h_{\mathcal{X}_N}\right)} \left| D_1^{\boldsymbol{\beta}} D_2^{\boldsymbol{\gamma}} \Phi(\boldsymbol{w}, \boldsymbol{z}) \right| \right).$$

The interpolation with a C^{2k} smooth kernel has approximation order k.

PUM and regular coverings

- Dealing with large data sets it is convenient to use the PUM. Its basic idea is to start with a partition of the open and bounded domain Ω into *d subdomains or patches* Ω_j, such that $\Omega \subseteq \cup_{j=1}^{d} \Omega_j$, with some mild overlap among them.

Definition

Suppose that $\Omega \subseteq \mathbb{R}^M$ is bounded and $\mathcal{X}_N = \{\boldsymbol{x}_i, i = 1, \ldots, N\} \subseteq \Omega$ is given. An open and bounded covering $\{\Omega_j\}_{j=1}^{d}$ is called regular for $(\Omega, \mathcal{X}_N)$ if the following properties are satisfied:

i. for each $\boldsymbol{x} \in \Omega$, the number of subdomains Ω_j, with $\boldsymbol{x} \in \Omega_j$, is bounded by a global constant C,

ii. each subdomain Ω_j satisfies an interior cone condition,

iii. the local fill distances $h_{\mathcal{X}_{N_j}}$ are uniformly bounded by the global fill distance $h_{\mathcal{X}_N}$, where $\mathcal{X}_{N_j} = \mathcal{X}_N \cap \Omega_j$.

PUM and locally supported weights

Definition

A family of compactly supported, non-negative and continuous functions $\{W_j\}_{j=1}^d$ is a k-stable partition of unity if

i. $\operatorname{supp}(W_j) \subseteq \Omega_j$,

ii. $\sum_{j=1}^d W_j(\boldsymbol{x}) = 1, \quad \boldsymbol{x} \in \Omega$,

iii. for every $\boldsymbol{\beta} \in \mathbb{N}^M$, with $|\boldsymbol{\beta}| \leq k$, there exists a constant $C_{\boldsymbol{\beta}} > 0$ such that

$$\left\| D^{\boldsymbol{\beta}} W_j \right\|_{L^\infty(\Omega_j)} \leq \frac{C_{\boldsymbol{\beta}}}{\left(\sup_{\boldsymbol{x},\boldsymbol{y} \in \Omega_j} \|\boldsymbol{x} - \boldsymbol{y}\|_2 \right)^{|\boldsymbol{\beta}|}}, \quad j = 1, \ldots, d.$$

RBF-PUM

- Then, for each subdomain Ω_j we consider a radial basis function R_j, as local interpolant and the global approximant is given by:

$$\mathcal{I}(\boldsymbol{x}) = \sum_{j=1}^{d} R_j(\boldsymbol{x}) W_j(\boldsymbol{x}), \quad \boldsymbol{x} \in \Omega.$$

- Thus, to find the PUM interpolant we need to solve d linear systems of the form $A_j \boldsymbol{c}_j = \boldsymbol{f}_j$, where $\boldsymbol{c}_j = (c_1^j, \ldots, c_{N_j}^j)^T$, $\boldsymbol{f}_j = (f_1^j, \ldots, f_{N_j}^j)^T$ and

$$(A_j)_{ik} = \phi(||\boldsymbol{x}_i^j - \boldsymbol{x}_k^j||_2), \quad \boldsymbol{x}_i^j \in \Omega_j, \quad i, k = 1, \ldots, N_j.$$

Error bounds for RBF-PU interpolants

Theorem

Let $\Omega \subseteq \mathbb{R}^M$ be open and bounded and $\mathcal{X}_N = \{\boldsymbol{x}_i, i = 1, \ldots, N\} \subseteq \Omega$. Let $\phi \in C_\nu^k(\mathbb{R}^M)$ be a strictly conditionally positive definite function of order L. Let $\{\Omega_j\}_{j=1}^d$ be a regular covering for $(\Omega, \mathcal{X}_N)$ and let $\{W_j\}_{j=1}^d$ be k-stable for $\{\Omega_j\}_{j=1}^d$. Then the error between $f \in \mathcal{N}_\phi(\Omega)$ and its PU interpolant can be bounded by

$$|D^\beta f(\boldsymbol{x}) - D^\beta \mathcal{I}(\boldsymbol{x})| \leq C' h_{\mathcal{X}_N}^{(k+\nu)/2-|\beta|} |f|_{\mathcal{N}_\phi(\Omega)},$$

for all $\boldsymbol{x} \in \Omega$ and all $|\beta| \leq k/2$.

Then, the partition of unity interpolant preserves the local approximation order for the global fit.

Essential references

On the efficiency of the PUM


G. Allasia, R. Besenghi, R. Cavoretto, A. De Rossi, *Scattered and track data interpolation using an efficient strip searching procedure*, Appl. Math. Comput. **217** (2011), 5949–5966.


S. Arya, D.M. Mount, N.S. Netanyahu, R. Silverman, A.Y. Wu, *An optimal algorithm for approximate nearest neighbor searching in fixed dimensions*, J. ACM **45** (1998), 891–923.


R. Cavoretto, A. De Rossi, *A trivariate interpolation algorithm using a cube-partition searching procedure*, SIAM J. Sci. Comput. **37** (2015), A1891–A1908.


R. Cavoretto, A. De Rossi, E. Perracchione, *Efficient computation of partition of unity interpolants through a block-based searching technique*, Comput. Math. Appl. **71** (2016), 2568–2584.


D.M. Mount, *ANN Programming Manual*, College Park, Maryland, 1998.


H. Wendland, *Surface reconstruction from unorganized points*, 2005, `http://people.maths.ox.ac.uk/wendland/research/old/reconhtml/reconhtml.html`

Statement of the problem

- In the PUM, the efficient organization of the scattered data among the subdomains turns out to be the crucial step.
- Techniques as *kd-trees*, which allow to partition data in a k-dimensional space have been designed.
- Here, we provide a partitioning structure, the so-called Sorting-based Partitioning Structure (S-PS), which is built ad hoc for the PUM with hyperspheres as patches.
- The set $\mathcal{X}_N$ is partitioned by a quicksort routine into q^M blocks. In this way, we obtain q^M subsets $\mathcal{X}_{N_k}$, where $\mathcal{X}_{N_k}$ are the points in the k-th neighborhood (composed by the k-th block and its $2^M - 1$ neighboring blocks).
- Here, $q = \lceil 1/\delta \rceil$, where $\delta = 1/d^{1/M}$ is the radius of patches and d is the number of PU subdomains. Moreover, d is so that $N/d \approx 4^M$ (see Figure 2).

The problem geometry

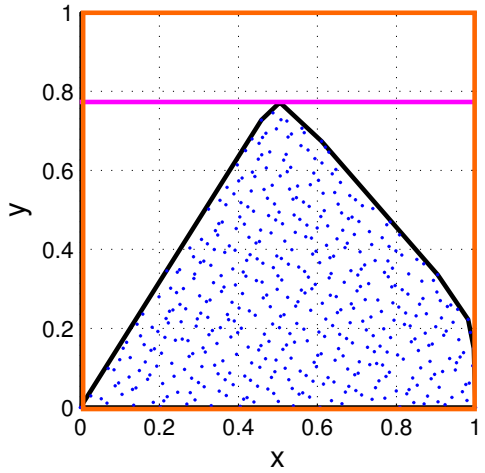

Figure 1: An example of the problem geometry in a 2D framework: the set of data sites $\mathcal{X}_N$ (blue), the convex hull Ω (black), the rectangle $\mathcal{R}$ containing Ω (pink) and the bounding box $\mathcal{L}$ (orange).

- The set of PU subdomain centres $\mathcal{C}_d = \{(\bar{x}_j, \bar{y}_j), j = 1, \ldots, d\}$ is constructed in Ω.
- $\mathcal{C}_d$ is obtained by building a grid of $d_{PU} = \left\lfloor \frac{1}{2} l_{box} \left(\frac{N}{A_K} \right)^{1/2} \right\rfloor^2$ points on $\mathcal{R}$. In this way the ratio $N/d \approx 4$ is preserved on Ω.

The sorting-based data structure

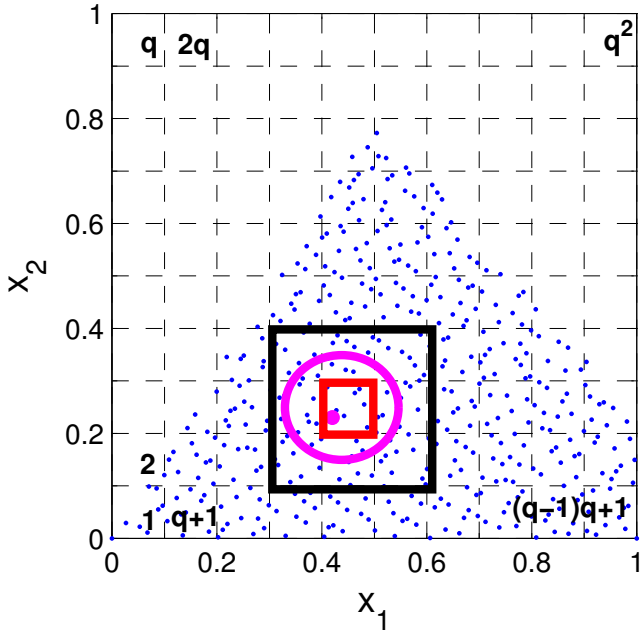

Figure 2: The k-th block (red), a subdomain centre belonging to the k-th block (pink) and the neighbourhood set (black).

- Given a PU centre $\bar{\boldsymbol{x}}_j$, if k_m is the index of the strip parallel to the subspace of dimension $M-1$ generated by x_p, $p = 1, \ldots, M$, and $p \neq m$, containing the m-th coordinate of $\bar{\boldsymbol{x}}_j$, then the index of the k-th block containing the PU centre is

$$k = \sum_{m=1}^{M-1} (k_m - 1)\, q^{M-m} + k_M.$$

Complexity analysis of the S-PS

- We summarize in Table 2 the complexity costs of the S-PS.

Table 2: Computational costs concerning the S-PS routine and the kd-tree one.

M	S-PS structure	kd-tree structure	S-PS search	kd-tree search
2	$\mathcal{O}(3/2N \log N)$	$\mathcal{O}(2N \log N)$	$\mathcal{O}(1)$	$\mathcal{O}(\log N)$
3	$\mathcal{O}(2N \log N)$	$\mathcal{O}(3N \log N)$	$\mathcal{O}(1)$	$\mathcal{O}(\log N)$

- Concerning the searching routine, for each subdomain a quicksort procedure which requires $\mathcal{O}(N_k \log N_k)$ time complexity is used to order distances. Moreover, observing that the data sites in a neighbourhood are about $N/(3q)^M$, we obtain:

$$\mathcal{O}\left(\frac{N}{3^M q^M} \log \frac{N}{3^M q^M}\right) \approx \mathcal{O}(1).$$

Numerical experiments I

- To point out the accuracy of our tests we will refer to the Maximum Absolute Error (MAE) and the Root Mean Square Error (RMSE):

$$MAE = \max_{1\le i\le s} |f(\tilde{\boldsymbol{x}}_i) - \mathcal{I}(\tilde{\boldsymbol{x}}_i)|, \quad RMSE = \sqrt{\frac{1}{s}\sum_{i=1}^{s} |f(\tilde{\boldsymbol{x}}_i) - \mathcal{I}(\tilde{\boldsymbol{x}}_i)|^2},$$

  where $\tilde{\boldsymbol{x}}_i$, $i = 1, \ldots, s$, are the evaluation points.
- We also compute the CPU times (refer to Tables 3–4) and two conditioning estimates, named the Maximum Conditioning number (MaxCond) and Average Conditioning number (AvCond):

$$MaxCond = \max_{1\le j\le d} cond(A_j), \qquad AvCond = \frac{1}{d}\sum_{j=1}^{d} cond(A_j),$$

- Tests are carried out considering the well-known 2D Franke's function and several sets of Halton data in a pentagonal region $\Omega \subseteq [0,1]^2$.

Numerical experiments II

Table 3: MAEs, RMSEs, MaxConds and AvConds for a pentagonal domain using the Franke's function as test function and the W2 function with $\varepsilon = 0.5$.

N	MAE	RMSE	MaxCond	AvCond
622	$1.65\mathrm{E}-03$	$1.40\mathrm{E}-04$	$1.30\mathrm{E}+07$	$7.12\mathrm{E}+06$
2499	$5.02\mathrm{E}-04$	$3.30\mathrm{E}-05$	$1.72\mathrm{E}+08$	$4.82\mathrm{E}+07$
9999	$4.33\mathrm{E}-05$	$6.33\mathrm{E}-06$	$1.92\mathrm{E}+09$	$5.46\mathrm{E}+08$
39991	$9.86\mathrm{E}-06$	$1.25\mathrm{E}-06$	$1.96\mathrm{E}+10$	$3.99\mathrm{E}+09$
159994	$1.67\mathrm{E}-06$	$3.05\mathrm{E}-07$	$1.74\mathrm{E}+11$	$3.56\mathrm{E}+10$

Numerical experiments II

- The CPU times obtained with the block-based partitioning structure are compared with the only full MATLAB implemented package for kd-trees, written by P. Vemulapalli, available at MATLAB central file exchange.

Table 4: CPU times obtained by running the S-PS and the kd-tree procedure.

N	622	2499	9999	39991	159994
t_{S-PS}	1.0	3.7	9.1	34.1	142.3
$t_{kd-tree}$	15.3	42.3	134.0	494.1	2013.88

Application to reconstruction of 3D objects

- The S-PS procedure works for 3D data sets and thus enables us to reconstruct 3D objects, refer to Figure 3 and Table 5.

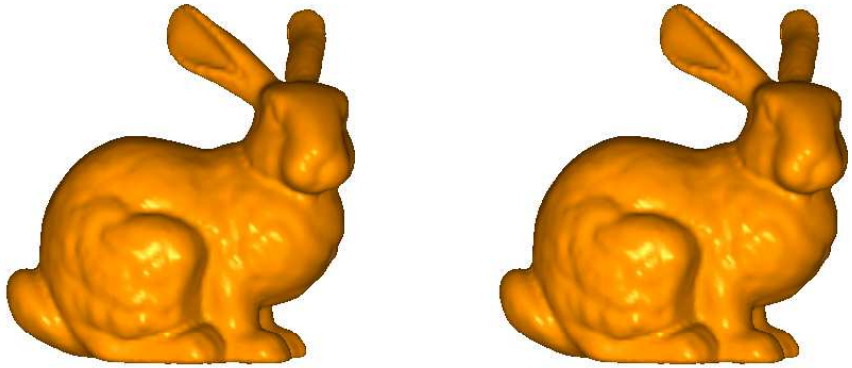

Figure 3: The Stanford Bunny with 8171 (left) and 35947 (right) data points.

Table 5: CPU times obtained by running the S-PS and the kd-tree procedure.

N	453	1889	8171	35947
t_{S-PS}	9.7	39.8	318.4	3881.9
$t_{kd-tree}$	144.8	589.5	3141.4	64909.8

The integer-based data structure

- The most expensive step in the S-PS is the computational cost of the sorting procedures used to order the data. This is also the reason why it can be applied only in low dimensions.
- However, we can avoid this drawback if we assign to each point the corresponding block by rounding off to an integer value.
- Precisely, given a PU centre, to find the indices k_m, $m = 1, \ldots, M$, of the strips to which it belongs, we use an Integer-based Partitioning Structure (I-PS) consisting in rounding off to an integer value. Thus, for each PU centre $\bar{\boldsymbol{x}}_j = (\bar{x}_{j1}, \ldots, \bar{x}_{jM})$, we have that

$$k_m = \left\lceil \frac{\bar{x}_{jm}}{\delta} \right\rceil.$$

- The I-PS turns out to be more efficient than the S-PS (refer to Table 6 and Figure 4).

Numerical experiments III

Table 6: CPU times (in seconds) obtained by running the sorting-based procedure (t_{S-PS}) and the integer-based one (t_{I-PS}).

N	25000	50000	100000	200000
t_{I-PS}	5.13	10.68	21.99	45.00
t_{S-PS}	5.21	12.40	28.77	71.55

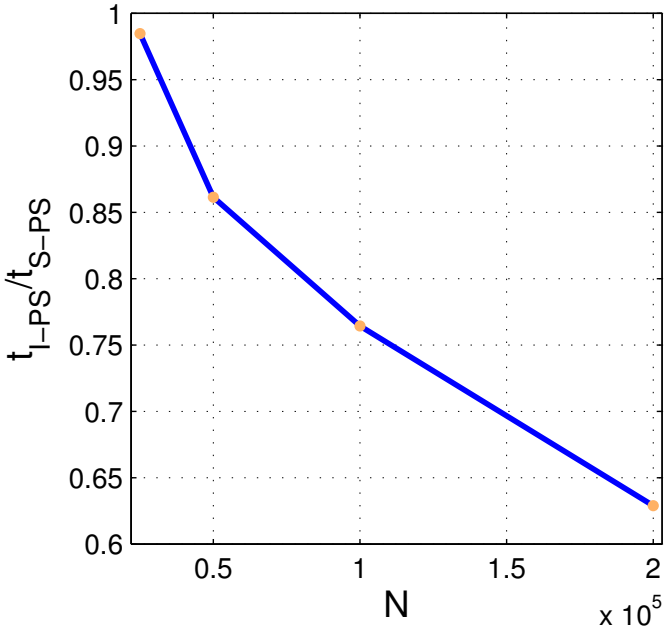

Figure 4: CPU time ratios t_{I-PS}/t_{S-PS} by varying N.

Essential references

On the accuracy of the PU method


R. Cavoretto, A. De Rossi, E. Perracchione, *Optimal selection of local approximants in RBF-PU interpolation*, to appear on J. Sci. Comput. (2017).


O. Davydov, *TSFIT: A software package for two-stage scattered data fitting*, 2009, `http://www.staff.uni-giessen.de/gc1266/t`.


S. Deparis, D. Forti, A. Quarteroni, *A rescaled and localized radial basis functions interpolation on non-cartesian and non-conforming grids*, SIAM J. Sci. Comput. **86** (2014), A2745–A2762.


G.E. Fasshauer, J.G. Zhang, *On choosing "optimal" shape parameters for RBF approximation*, Numer. Algorithms **45** (2007), 345–368.


A. Safdari-Vaighani, A. Heryudono, E. Larsson, *A radial basis function partition of unity collocation method for convection-diffusion equations arising in financial applications*, J. Sci. Comput. **64** (2015), 341–367.


S. Rippa, *An algorithm for selecting a good value for the parameter c in radial basis function interpolation*, Adv. Comput. Math. **11** (1999), 193–210.

Statement of the problem

- The local basis functions are defined in function of a shape parameter which greatly affects the accuracy of the local interpolants.
- Many researchers already worked on the problem of finding suitable values for the shape parameter in order to avoid problems of instability.
- However, in the PU method also the sizes of the local systems play a crucial role for the final outcome.
- Focusing on hyperspherical patches, our aim consists in developing a method which enables us to select both suitable sizes of the different PU subdomains and shape parameters, i.e. to choose $(\delta_j, \varepsilon_j)$, where δ_j is the PU radius and ε_j is the shape parameter.

Optimal local RBF approximants

- Among several techniques for selecting the optimal shape parameter, we focus on the so-called Leave One Out Cross Validation (LOOCV), properly modified for a bivariate optimization problem (BLOOCV).
- For a fixed $i \in \{1, \dots, N_j\}$, let

$$R_j^{(i)}(\boldsymbol{x}) = \sum_{k=1, k\neq i}^{N_j} c_k^j \phi(||\boldsymbol{x} - \boldsymbol{x}_k^j||_2) \quad \text{and} \quad e_i^j = f_i^j - R_j^{(i)}(\boldsymbol{x}_i^j),$$

be respectively the j-th interpolant obtained leaving out the i-th data on Ω_j and the error at the i-th point.

- The computation of the error can be simplified by calculating

$$e_i^j = \frac{c_i^j}{(A_j)_{ii}^{-1}},$$

where c_i^j is the i-th coefficient of R_j, based on the full data set.

The BLOOCV-PU approximant

- Thus, in order to obtain an error estimate, we compute the vector $\boldsymbol{e}_j(\delta_j, \varepsilon_j) = (e_1^j, \ldots, e_{N_j}^j)$.
- Then, focusing on $||\cdot||_\infty$, we compute $\boldsymbol{e}_j$ for several values $(\delta_{j_1}, \ldots, \delta_{j_P})$ and $(\varepsilon_{j_1}, \ldots, \varepsilon_{j_Q})$, i.e. we provide

$$E_j = \begin{pmatrix} ||\boldsymbol{e}_j(\delta_{j_1}, \varepsilon_{j_1})||_\infty & \cdots & ||\boldsymbol{e}_j(\delta_{j_1}, \varepsilon_{j_Q})||_\infty \\ \vdots & \ddots & \vdots \\ ||\boldsymbol{e}_j(\delta_{j_P}, \varepsilon_{j_1})||_\infty & \cdots & ||\boldsymbol{e}_j(\delta_{j_P}, \varepsilon_{j_Q})||_\infty \end{pmatrix}.$$

- The j-th local approximant is computed considering the couple $(\delta_j, \varepsilon_j)$ if $||\boldsymbol{e}_j(\delta_j, \varepsilon_j)||_\infty = \min_{p=1,\ldots,P}(\min_{q=1,\ldots,Q}(E_j)_{pq})$. Denoting by $N_j(\delta_j)$ the number of points on Ω_j of radius δ_j, the BLOOCV-PU is given by

$$\tilde{\mathcal{I}}(\boldsymbol{x}) = \sum_{j=1}^{d} \sum_{k=1}^{N_j(\delta_j)} c_k^j \phi_{\varepsilon_j}(||\boldsymbol{x} - \boldsymbol{x}_k^j||_2) W_j(\boldsymbol{x}), \quad \boldsymbol{x} \in \Omega.$$

Numerical experiments I

- To test the accuracy, we compute MAE and RMSE (refer to Table 7).
- Tests are carried out considering the so-called *valley function*

$$f(x_1, x_2) = \frac{1}{2} x_2 \left[\cos(4x_1^2 + x_2^2 - 1)\right]^4.$$

- We use both Halton data and non-conformal points (see Figure 5).

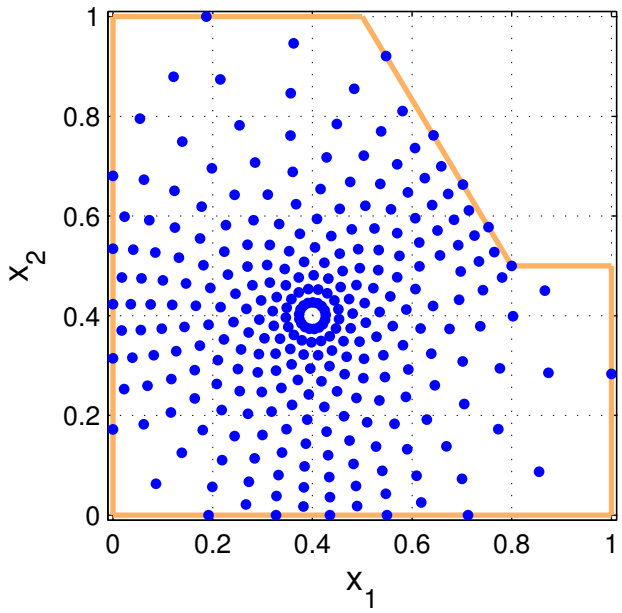

Figure 5: Example of 289 Non-Conformal points (NC).

Numerical experiments II

N	Method	RMSE H	MAE H	RMSE NC	MAE NC
289	PU	$2.59\mathrm{E}-02$	$4.30\mathrm{E}-01$	$5.30\mathrm{E}-02$	$5.00\mathrm{E}-01$
	BLOOCV-PU	$1.32\mathrm{E}-02$	$2.76\mathrm{E}-01$	$3.47\mathrm{E}-02$	$3.13\mathrm{E}-01$
1089	PU	$3.51\mathrm{E}-03$	$6.20\mathrm{E}-02$	$3.90\mathrm{E}-02$	$5.00\mathrm{E}-01$
	BLOOCV-PU	$2.11\mathrm{E}-04$	$8.93\mathrm{E}-03$	$7.11\mathrm{E}-03$	$8.38\mathrm{E}-02$
4225	PU	$8.63\mathrm{E}-04$	$2.00\mathrm{E}-02$	$4.63\mathrm{E}-02$	$4.99\mathrm{E}-01$
	BLOOCV-PU	$3.88\mathrm{E}-06$	$1.12\mathrm{E}-04$	$2.39\mathrm{E}-03$	$4.77\mathrm{E}-02$
16641	PU	$4.07\mathrm{E}-04$	$1.18\mathrm{E}-02$	$4.34\mathrm{E}-02$	$5.00\mathrm{E}-01$
	BLOOCV-PU	$8.26\mathrm{E}-08$	$2.80\mathrm{E}-06$	$7.51\mathrm{E}-04$	$8.10\mathrm{E}-03$
66049	PU	$1.23\mathrm{E}-04$	$4.19\mathrm{E}-03$	$4.03\mathrm{E}-02$	$5.00\mathrm{E}-01$
	BLOOCV-PU	$5.10\mathrm{E}-08$	$1.76\mathrm{E}-06$	$8.28\mathrm{E}-05$	$1.27\mathrm{E}-03$

Table 7: RMSEs and MAEs computed with the IMQ for Halton points and with the W6 for the Non-Conformal points.

Application to Earth's topography

- We consider the *black forest* data set. It consists of 15885 points representing a terrain in the neighborhood of Freiburg, Germany.
- The difference between the maximal and minimal heights is 1214 m.
- We use as local approximant the M2 function (see Figure 6).

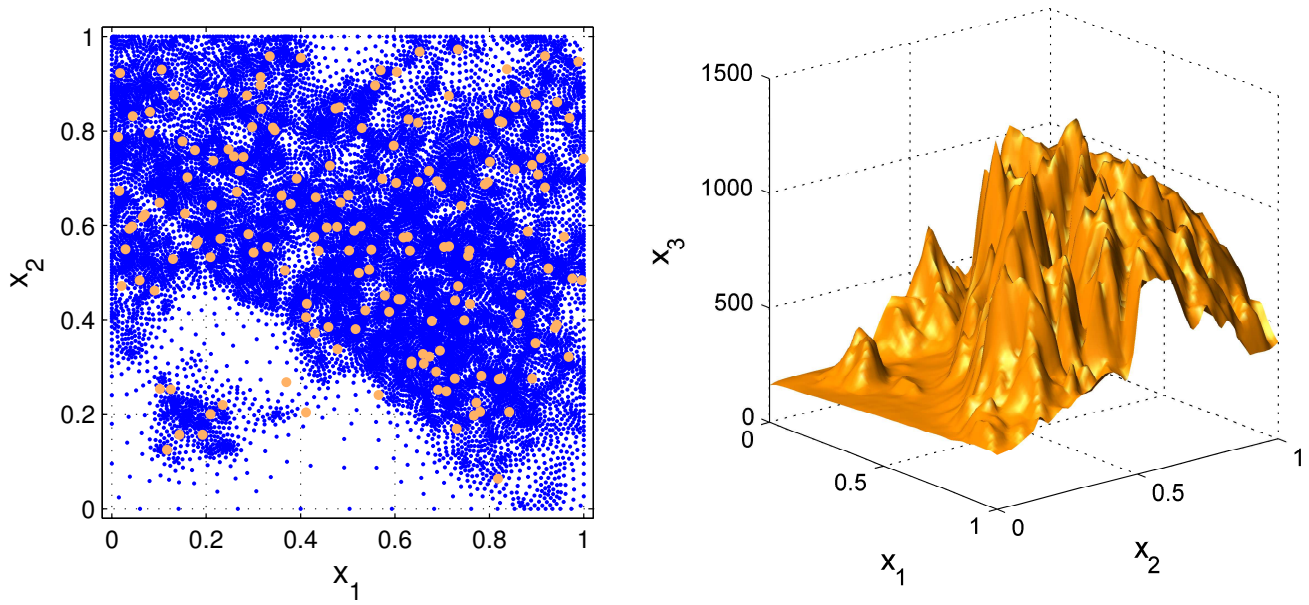

Figure 6: Left: a 2D view of the black forest data set. Right: graphical approximation of the black forest data set. We obtain RMSE= 5.73 m, MAE= 26.0 m, MRE= 0.021.

Essential references

On the positivity of the PU method


M.R. Asim, G. Mustafa, K. Brodlie, *Constrained visualization of 2D positive data using modified quadratic Shepard method*, in: V. Skala (Ed.), WSCG 2004: The 12-th International Conference in Central Europe on Computer Graphics, Visualization and Computer Vision, vol. 27, 2004, 469–485.


A. De Rossi, E. Perracchione, *Positive constrained approximation via RBF-based partition of unity method*, J. Comput. Appl. Math. **319** (2017), 338–351.


M.Z. Hussain, M. Sarfraz, *Positivity-preserving interpolation of positive data by rational cubics*, J. Comput. Appl. Math. **218** (2008), 446–458.


J.W. Schmidt, W. Hess, *Positivity of cubic polynomials on intervals and positive spline interpolation*, BIT **28** (1998), 340–352.


Z. Wu, R. Schaback, *Shape preserving interpolation with radial basis function*, Acta Math. Appl. Sinica **10** (1994), 443–448.


J. Wu, X. Zhang, L. Peng, *Positive approximation and interpolation using compactly supported radial basis functions*, Math. Probl. Eng. **2010** (2010), 1–10.

Statement of the problem

- Dealing with applications, we often have additional properties, such as the positivity of the measurements, which we wish to be preserved during the interpolation process.
- The positivity-preserving problem has been studied in particular cases (e.g. for TPSs or MQ quasi-interpolation).
- Moreover, such problem has been considered for CSRBFs. Precisely, a global positive approximant obtained by adding up several positive constraints has already been designed.
- However, since a global interpolant is used, adding up other constraints to preserve the positivity implies that the shape of the fit is consequently globally modified.
- This might lead to a considerable decrease of the quality of the approximating function in comparison with the unconstrained CSRBF interpolation.

Positive local RBF approximants

- In order to avoid such drawback, we can perform a local implementation.
- Sufficient condition to have positive approximants on Ω_j is that the coefficients c_k^j are all positive. To such scope, on the subdomain Ω_j we choose a set of $\hat{N}_j$ added data $\mathcal{X}_{\hat{N}_j} = \{\hat{\boldsymbol{x}}_i^j, i = N_j + 1, \ldots, N_j + \hat{N}_j\}$.
- Then, the j-th problem consists in finding $\hat{R}_j$ of the form

$$\hat{R}_j(\boldsymbol{x}) = \sum_{k=1}^{N_j} c_k^j \phi_\varepsilon(||\boldsymbol{x} - \boldsymbol{x}_k^j||_2) + \sum_{\hat{k}=N_j+1}^{N_j+\hat{N}_j} c_{\hat{k}}^j \hat{\phi}_{\varepsilon_{\hat{k}}}(||\boldsymbol{x} - \hat{\boldsymbol{x}}_{\hat{k}}^j||_2),$$

such that

$$\hat{R}_j(\boldsymbol{x}_i^j) = f_i^j, \quad i = 1, \ldots, N_j, \quad c_i^j \geq 0, \quad i = 1, \ldots, N_j + \hat{N}_j,$$

where $\hat{\phi}_{\varepsilon_{\hat{k}}}$ are CSRBFs (of different supports).

The PC-PU approximant

- The reason for which we consider (for the added nodes) different supports for the CSRBFs follows from the fact that, if they are properly chosen, we can ensure that the problem admits solution (in the special case for which $\hat{N}_j = N_j$).
- In practical use, the aim is to add few data. Thus, we select via LOOCV the optimal number of added data $\hat{N}_j$ which yields maximal accuracy and ensures the positivity of the local interpolant.
- Therefore, for each subdomain we select a suitable number of constraints $\hat{N}_j$, which can also be 0, and the Positive Constrained PU (PC-PU) approximant assumes the form

$$\hat{\mathcal{I}}(\boldsymbol{x}) = \sum_{j=1}^{d} \left(\sum_{k=1}^{N_j} c_k^j \phi_\varepsilon(||\boldsymbol{x} - \boldsymbol{x}_k^j||_2) + \sum_{\hat{k}=N_j+1}^{N_j+\hat{N}_j} c_{\hat{k}}^j \hat{\phi}_{\varepsilon_{\hat{k}}}(||\boldsymbol{x} - \hat{\boldsymbol{x}}_{\hat{k}}^j||_2) \right) W_j(\boldsymbol{x}).$$

Numerical experiments I

- Tests are performed considering different sets of random points (see Table 8) and the following test function

$$f_1(x_1, x_2) = (x_1 - 0.5)^2 + (x_2 - 0.4)^2.$$

- We consider the W2 function for the added nodes and both the W2 and IMQ functions for the given interpolation conditions.

Numerical experiments II

N	Method	MAE W2	RMSE W2	MAE IMQ	RMSE IMQ
300	PU	$1.50\mathrm{E}-01$	$1.52\mathrm{E}-02$	$1.39\mathrm{E}-01$	$1.04\mathrm{E}-02$
	PC-PU	$1.50\mathrm{E}-01$	$2.03\mathrm{E}-02$	$1.39\mathrm{E}-01$	$1.44\mathrm{E}-02$
1000	PU	$7.36\mathrm{E}-02$	$3.08\mathrm{E}-03$	$7.02\mathrm{E}-02$	$2.88\mathrm{E}-03$
	PC-PU	$7.96\mathrm{E}-02$	$6.44\mathrm{E}-03$	$7.02\mathrm{E}-02$	$3.49\mathrm{E}-03$
3500	PU	$6.34\mathrm{E}-02$	$1.47\mathrm{E}-03$	$5.89\mathrm{E}-02$	$1.50\mathrm{E}-03$
	PC-PU	$8.40\mathrm{E}-02$	$2.86\mathrm{E}-03$	$5.89\mathrm{E}-02$	$1.66\mathrm{E}-03$
8000	PU	$2.43\mathrm{E}-02$	$4.17\mathrm{E}-04$	$2.33\mathrm{E}-02$	$3.46\mathrm{E}-04$
	PC-PU	$5.99\mathrm{E}-02$	$1.03\mathrm{E}-03$	$2.33\mathrm{E}-02$	$3.68\mathrm{E}-04$

Table 8: RMSEs and MAEs computed with the W2 and IMQ kernels for random points.

Essential references

On the stability of the PU method


R. Cavoretto, S. De Marchi, A. De Rossi, E. Perracchione, G. Santin, *Partition of unity interpolation using stable kernel-based techniques*, Appl. Numer. Math. **116** (2017), 95–107.


R. Cavoretto, G.E. Fasshauer, M. McCourt, *An introduction to the Hilbert-Schmidt SVD using iterated Brownian bridge kernels*, Numer. Algorithms **68** (2015), 393–422.


S. De Marchi, G. Santin, *Fast computation of orthonormal basis for RBF spaces through Krylov space methods*, BIT **55** (2015), 949–966.


B. Fornberg, E. Larsson, N. Flyer, *Stable computations with Gaussian radial basis functions*, SIAM J. Sci. Comput. **33** (2011), 869–892.


B. Fornberg, E. Lehto, *Stabilization of RBF-generated finite difference methods for convective PDEs*, J. Comput. Phys. **230** (2011), 2270–2285.


M. Pazouki, R. Schaback, *Bases for kernel-based spaces*, J. Comput. Appl. Math. **236** (2011), 575–588.

Statement of the problem

- In some cases, the local approximants and consequently also the global one may suffer from instability due to ill-conditioning of the interpolation matrices. This is particularly evident when the shape parameter $\varepsilon \longrightarrow 0$.
- For particular RBFs, techniques allowing to stably and accurately compute the interpolant, such as RBF-QR methods, have already been designed.
- A more general approach, consisting in computing via a truncated Singular Value Decomposition (SVD) stable bases, namely Weighted SVD (WSVD) bases, is here coupled with the PU method.
- The resulting approach, namely WSVD-PU method, is stable and accurate. Indeed, while in the global case a large number of truncated terms of the SVD must be dropped to preserve stability, a local technique requires only few terms are eliminated.

Stable local RBF approximants

The theoretical background of the WSVD bases lies in the following,

Theorem (Mercer's Theorem)

If the kernel Φ is continuous and positive definite on a bounded set $\Omega \subseteq \mathbb{R}^M$, the operator $T : L_2(\Omega) \to L_2(\Omega)$,

$$T[f](\boldsymbol{x}) = \int_\Omega \Phi(\boldsymbol{x}, \boldsymbol{y}) f(\boldsymbol{y}) d\boldsymbol{y},$$

has a countable set of eigenfunctions $\{\varphi_k\}_k$ and eigenvalues $\{\lambda_k\}_k$. The eigenfunctions are orthonormal in $L_2(\Omega)$ and orthogonal in $\mathcal{N}_\Phi(\Omega)$ with $\|\varphi_k\|^2_{\mathcal{N}_\Phi(\Omega)} = \lambda_k^{-1}$. Moreover, the kernel can be expressed in terms of the eigencouples as

$$\Phi(\boldsymbol{x}, \boldsymbol{y}) = \sum_k \lambda_k \varphi_k(\boldsymbol{x}) \varphi_k(\boldsymbol{y}), \ \boldsymbol{x}, \boldsymbol{y} \in \Omega.$$

The WSVD-PU approximant

- The so-constructed WSVD basis $\{u_k\}_{k=1}^{N}$ has the following property:

$$(u_k, f)_{\ell_2(\mathcal{X}_N)} = \sigma_k (u_k, f)_{\mathcal{N}_\Phi(\Omega)}, \quad \forall f \in \mathcal{N}_\Phi(\Omega),$$

- Therefore, the local interpolants can be rewritten as

$$\bar{R}_j^{N_j}(\boldsymbol{x}) = \sum_{k=1}^{N_j} (\sigma_k^j)^{-1} (f_{|\Omega_j}, u_k^j)_{\ell_2(\mathcal{X}_{N_j})} u_k^j(\boldsymbol{x}).$$

  If we instead solve the problem over $\operatorname{span}\{u_1^j, \ldots, u_{m_j}^j\}$, $m_j \leq N_j$, we find a solution given by the truncation of the local interpolants, i.e.

$$\bar{\mathcal{I}}(\boldsymbol{x}) = \sum_{j=1}^{d} \bar{R}_j^{m_j}(\boldsymbol{x}) W_j(\boldsymbol{x}), \quad \boldsymbol{x} \in \Omega.$$

- Thus, for each Ω_j a SVD is performed and then we leave out the $N_j - m_j$ terms which are less than or equal to a prescribed tolerance τ. This can be efficiently carried out with Krylov space methods.

Numerical experiments I

- Tests are carried out by computing the RMSE for the Franke's function and for different values of the shape parameter ε in the range $[10^{-3}, 10^{2}]$, refer to Figures 7–8.

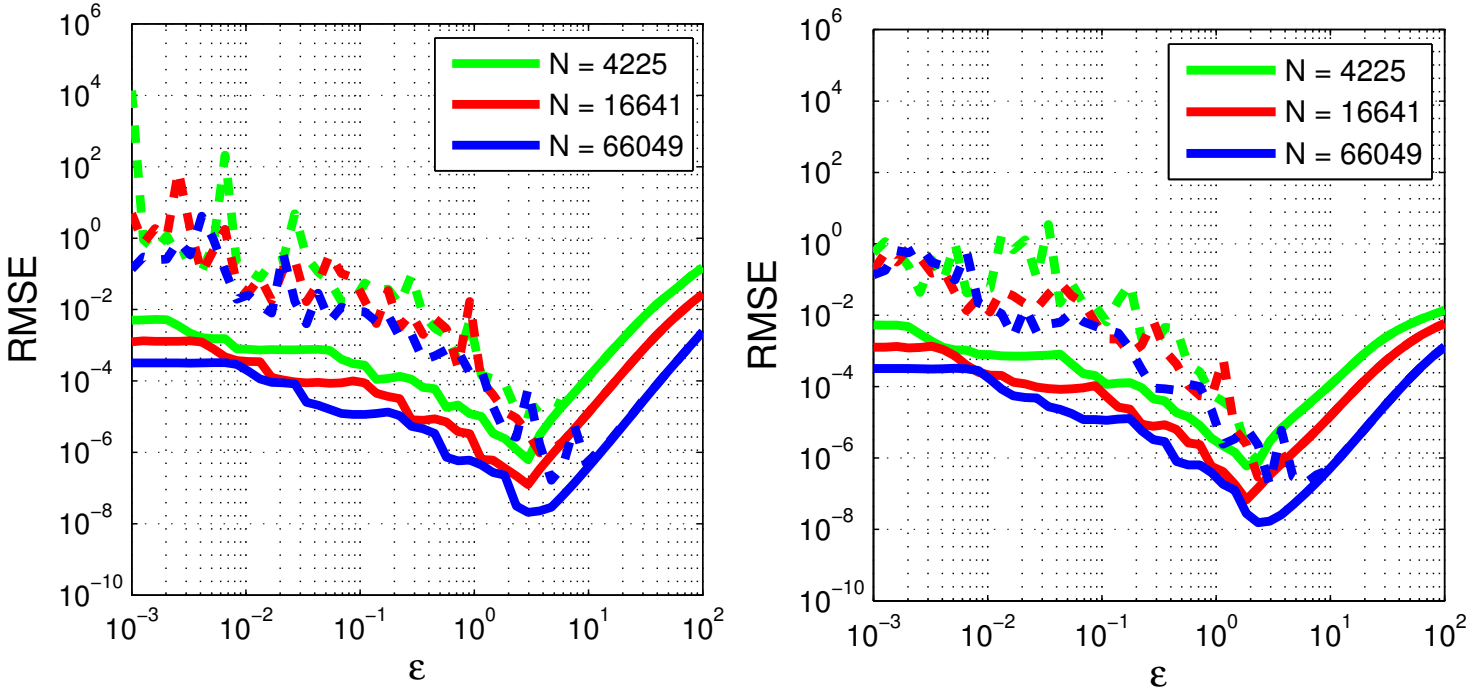

Figure 7: RMSEs obtained by varying ε for C^∞ kernels. The classical PU interpolant is plotted with dashed line and the WSVD-PU approximant with solid line. From left to right, we consider the G and IMQ C^∞ kernels.

Numerical experiments II

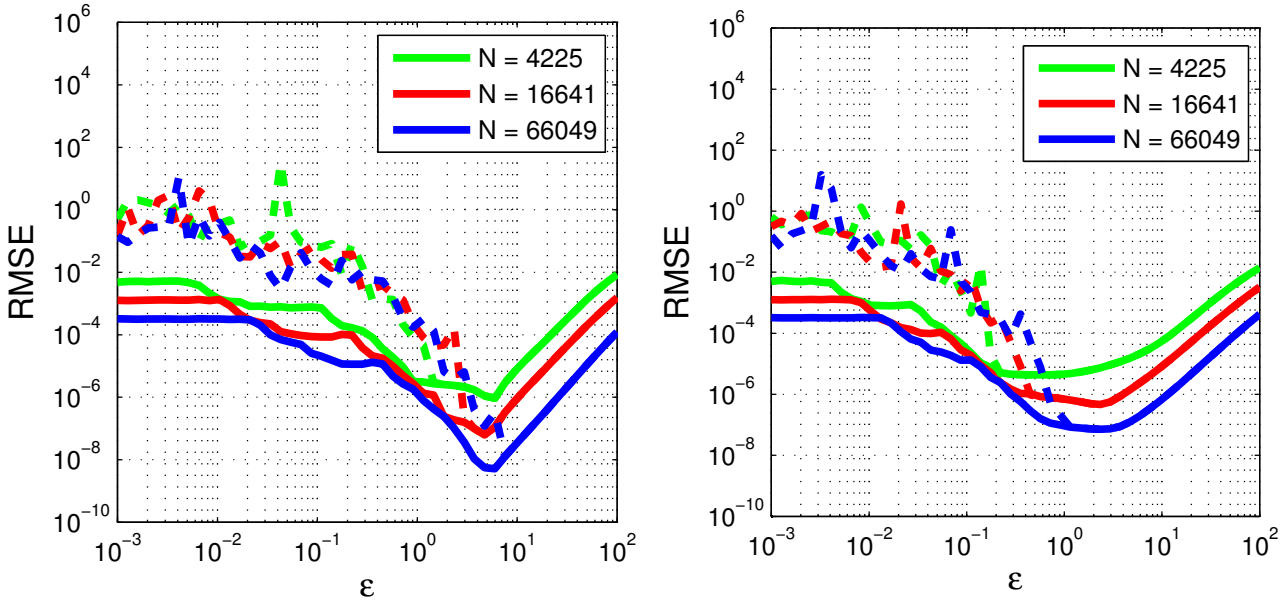

Figure 8: RMSEs obtained by varying ε for the M6 and M4 kernels, left and right respectively.

The differences between the PU and WSVD-PU can be summarized as:

i. C^∞ RBFs: improvement of stability and of the optimal accuracy,

ii. C^k RBFs, $k \geq 1$: improvement of stability and same optimal accuracy,

iii. C^0 RBFs: same stability and same optimal accuracy.

Essential references

Approximation of track data via PUM


R. Cavoretto, A. De Rossi, E. Perracchione, *Optimal selection of local approximants in RBF-PU interpolation*, to appear on J. Sci. Comput (2017).


G.E. Fasshauer, M.J. McCourt, *Kernel-based Approximation Methods Using* MATLAB, World Scientific, Singapore, 2015.


B. Fornberg, E. Larsson, N. Flyer, *Stable computations with Gaussian radial basis functions*, SIAM J. Sci. Comput. **33** (2011), 869–892.


O. Kounchev, *Multivariate Polysplines. Applications to Numerical and Wavelet Analysis*, Academic Press/currently Elsevier, 2001.


S. Rippa, *An algorithm for selecting a good value for the parameter c in radial basis function interpolation*, Adv. Comput. Math. **11** (1999), 193–210.


H. Wendland, *Scattered Data Approximation*, Cambridge Monogr. Appl. Comput. Math., vol. 17, Cambridge Univ. Press, Cambridge, 2005.

State of the art, motivations and targets

- For the PUM both the sizes and shapes of the local subdomain play a crucial role for the final outcome. Ellipsoidal patches seem to be suitable, in particular for track data.
- Furthermore, in that case the choice of anisotropic kernels naturally follows. Any isotropic radial kernel can be turned into an anisotropic one by using a weighted 2-norm instead of an unweighted one.
- Focusing on ellipsoidal patches, our aim consists in developing a method which enables us to select both suitable sizes of the different PU subdomains and shape parameters, i.e. suitable local approximants.

The general framework

- In practice, for each subdomain Ω_j, the aim consists in selecting the shape parameters ε_j and semi-axes of the ellipsoidal patches $\boldsymbol{\delta}_j$.
- We will focus on the cross-validation algorithm, properly modified for a multivariate optimization problem.
- For a fixed $i \in \{1, \dots, N_j\}$, let

$$R_j^{(i)}(\boldsymbol{x}) = \sum_{k=1, k\neq i}^{N_j} c_k^j \phi(||\boldsymbol{x} - \boldsymbol{x}_k^j||_2) \quad \text{and} \quad e_i^j = f_i^j - R_j^{(i)}(\boldsymbol{x}_i^j),$$

be respectively the j-th interpolant obtained leaving out the i-th data on Ω_j and the error at the i-th point.

Local error estimates

- The computation of the error can be simplified by calculating

$$E_j(\boldsymbol{\varepsilon_j}, \boldsymbol{\delta_j}) = ||(e_1^j, \ldots, e_{N_j}^j)||_p = \left|\left| \left(\frac{c_1^j}{(A_j)_{11}^{-1}}, \ldots, \frac{c_{N_j}^j}{(A_j)_{N_j N_j}^{-1}} \right) \right|\right|_p,$$

  where c_i^j is the i-th coefficient of the RBF interpolant R_j based on the full data set and $(A_j)_{ii}^{-1}$ is the i-th diagonal element of the inverse of the corresponding local interpolation matrix.

Remark

A natural choice for optimizing the local RBF interpolants consists in computing error estimates for several values of the semi-axes and of the shape parameters. Here, we speed up this procedure via multivariate derivative-free optimization tools. In particular, for the implementation we use the MATLAB *software and the* `fminsearch.m` *routine.*

Properties of the covering and weights

- After optimizing the parameters $(\varepsilon_j, \boldsymbol{\delta}_j)$, we have a PU covering, made of ellipsoids, that satisfy interior cone conditions, indeed:

Proposition (cf. Wendland (2005), Proposition 11.26, p. 195)

If D is bounded, star-shaped with respect to $B(\boldsymbol{x}_c, \rho)$, and contained in $B(\boldsymbol{x}_c, \rho^*)$ then D satisfies an interior cone condition with radius ρ and angle $\theta = 2\arcsin[\rho/(2\rho^*)]$.

- As weight functions, we select the *Shepard's weights*

$$W_j(\boldsymbol{x}) = \bar{W}_j(\boldsymbol{x}) \Big/ \sum_{k=1}^{d} \bar{W}_k(\boldsymbol{x}), \quad j = 1, \ldots, d,$$

where $\bar{W}_j$ are anisotropic Wendland's functions. In fact, the shape parameters are selected so that $\mathrm{supp}(\bar{W}_j) = \Omega_j$.

Numerical experiments

- To test the accuracy, we compute MAE and RMSE for the well-known *2D Franke's function*.
- For the local approximants we take the anisotropic IMQ C^∞ kernel and for the PU weights the anisotropic Wendland's C^2 function.
- We use track data (see Figure 9) and the centres of the patches are constructed as a grid of t^2 points on Ω, where t is the number of tracks.

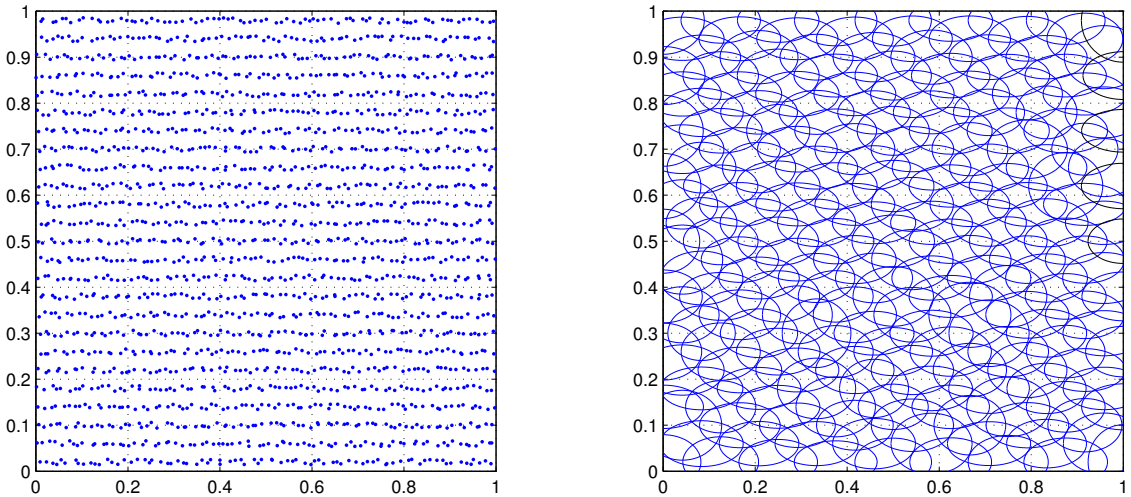

Figure 9: Left: a set of 2000 track data (25 tracks with 80 data points). Right: an illustrative example that shows how patches are selected.

Results and comparisons

N	Method	RMSE	MAE	CPU
1000 (20×50)	PU-LOOCV	$8.02\mathrm{E}-5$	$1.56\mathrm{E}-3$	76.6
	PU	$8.34\mathrm{E}-4$	$7.93\mathrm{E}-3$	1.78
2000 (25×80)	PU-LOOCV	$2.58\mathrm{E}-5$	$3.33\mathrm{E}-4$	119
	PU	$1.16\mathrm{E}-4$	$3.29\mathrm{E}-3$	3.88
4000 (40×100)	PU-LOOCV	$4.76\mathrm{E}-6$	$8.70\mathrm{E}-5$	182
	PU	$1.43\mathrm{E}-3$	$4.28\mathrm{E}-2$	22.2
8000 (50×160)	PU-LOOCV	$1.25\mathrm{E}-6$	$2.77\mathrm{E}-5$	290
	PU	$1.72\mathrm{E}-4$	$3.14\mathrm{E}-3$	53.9
16000 (80×200)	PU-LOOCV	$4.55\mathrm{E}-7$	$6.14\mathrm{E}-6$	651
	PU	$4.24\mathrm{E}-4$	$4.95\mathrm{E}-3$	229

Application to Earth's topography

- To test the method with real data, we consider points extracted from maps and specifically the Korea's map (see Figure 10).
- This example is particularly suitable because, even if we deal with real data, we can consider an arbitrary number of evaluation points to test the fit.
- We use as local approximants the Matérn M0 and M2.

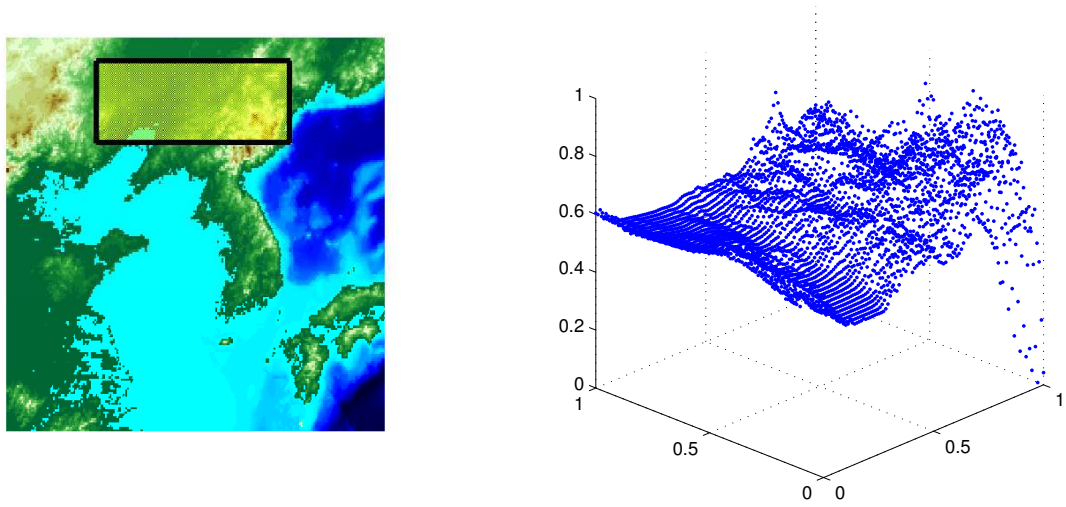

Figure 10: Left: the Korea's map and the extracted tracks. Right: a 3D view of the data set.

Application to Earth's topography

- The results are shown in Figure 11 and in Table 9.

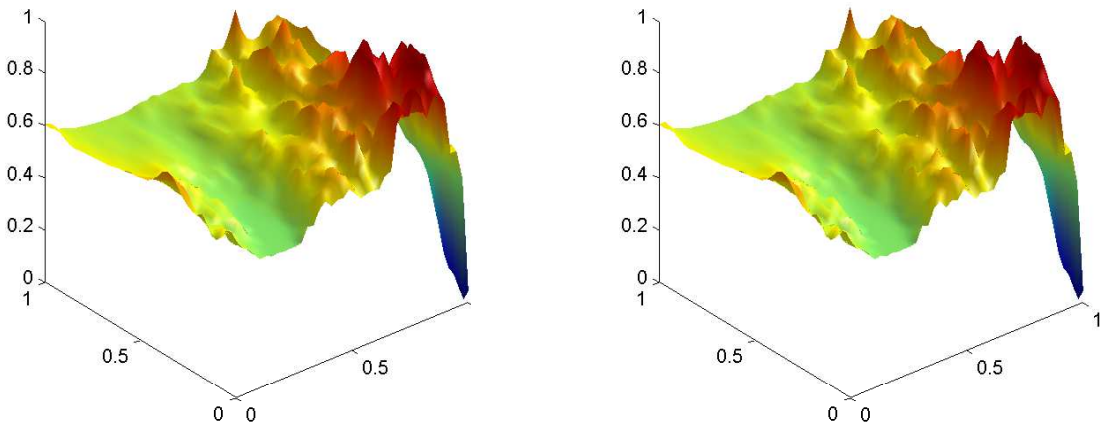

Figure 11: The reconstructed surfaces obtained by using the M0 (left) and M2 (right) kernels.

N	RBF	RMSE	MAE
4000 (40×100)	M0	$9.71\mathrm{E}-3$	$1.91\mathrm{E}-1$
	M2	$5.32\mathrm{E}-3$	$6.91\mathrm{E}-2$

Table 9: RMSEs and MAEs obtained by using the anisotropic Matérn kernels for the Korea data set.

Conclusions

- PUM allows to overcome the high computational cost associated to the global RBF method. Its efficiency can be improved with the use of ad hoc partitioning structures. Furthermore, we provide numerical tools that enable us to compute stable and accurate PU approximants, which can also satisfy the positivity property.
- Work in progress: Our aim is to provide a tool enabling us to select, for each PU subdomain, both its sizes and shape parameters. Numerical experiments with real world measurements shows that the proposed method accurately fits track data with highly varying densities. Moreover, the implementation is carried out with a new multivariate optimization procedure.

Conclusions

Thank you for the attention!